Inorganic Chemistry

Article

pubs.acs.org/IC

Syntheses and Structures of Closely Related Copper(I) Complexes of Tridentate (2-Pyridylmethyl)imine and (2-Pyridylmethyl)amine Ligands and Their Use in Mediating Atom Transfer Radical Polymerizations

Sara A. Turner,[†] Zachary D. Remillard,[†] Desire T. Gijima,[†] Emily Gao,[†] Robert D. Pike,[‡] and Christopher Goh*[,†]

[†]Department of Chemistry, Williams College, Williamstown, Massachusetts 01267, United States

[‡]Department of Chemistry, College of William and Mary, Williamsburg, Virginia 23187, United States

Supporting Information

ABSTRACT: A series of five copper(I) bromide complexes of tridentate (N,N,L) pyridine−imine and pyridine−amine ligands with a third amine, ether, or thioether neutral donor was synthesized and utilized in the atom transfer radical polymerization of styrene. The ligand design illustrated a systematic approach to the development of copper complexes for use in ATRP. Variations in the nature of the ligand impacted the solid state structures of the complexes. A mononuclear [CuBr(L)] complex was observed for L = pyridine−amine−amine, whereas complexes of L = pyridine−imine−amine and −thioether formed dinuclear $[CuBr(L)]_2$ structures with a central 10-membered ring. A doubly-bromide-bridged dimer was revealed for the [CuBr(L)] complex of L = pyridine−imine−ether and a polymeric species for [CuBr(L)], where L = pyridine−imine−amine and the imine−amine spacer was extended from two to three carbon atoms. In the application of these complexes to the ATRP of styrene, the redox potentials of the complexes were found to be one indicator of ATRP efficiency. Of the series presented, two complexes in particular provided fast polymerization rates and good to excellent molecular weight control. In both of these complexes, the ligand contained all nitrogen-based donor moieties.

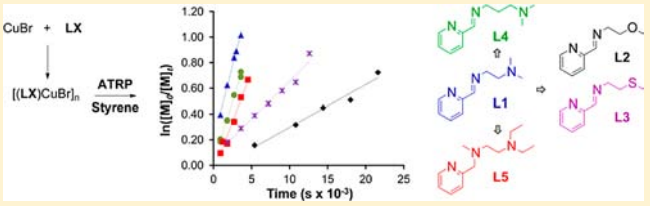

INTRODUCTION

Copper complexes of ligands containing pyridine, imine, and amine moieties have found multiple applications in metal-catalyzed processes. Examples include catalysts for polymerizations and organic transformations,[1−5] model complexes in the biomimetic study of copper proteins,[6] antimicrobial agents,[7] and components for design of magnetic materials.[8] Recent attention has also focused on their potential use in metal-based processes in neurodegenerative diseases such as Alzheimer's.[9] Our group has been interested in the use of such neutral tridentate pyridine−imine ligands with varying third donor moieties in metal-mediated atom transfer radical polymerization (ATRP). This polymerization technique provides the power to dictate the composition, functionality, molecular weight, and precise architecture of macromolecules.[10,11] Its use has led to extraordinary creativity in the design of macromolecules of tailored compositions and topologies and an unprecedented exploration of applications, including materials for biomedical applications, composite, and electronic materials.[10,12] Central to the basic mechanism of ATRP is the establishment of a fast and dynamic halide exchange process between growing and dormant polymer chains and a metal complex during polymerization (Figure 1). This process lowers the concentration of active radical chain ends to an extent that radical−radical termination reactions are suppressed and control over chain growth is established. In addition, isolation

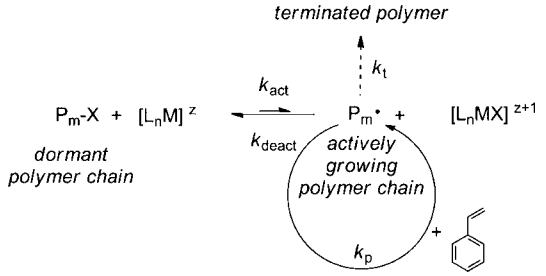

Figure 1. Redox equilibrium between dormant polymer chain and reduced metal complex and active growing polymer and oxidized metal complex governing the control of styrene polymer growth (P_m−X is dormant polymer chain, $[L_nM]^z$ is the reduced form of generic metal−ligand complex of charge z, P_m· is the active polymer chain, $[L_nMX]^{z+1}$ is the generic metal−ligand−halide complex of charge $z + 1$, and k_{act}, k_{deact}, k_p, and k_t are rate constants of polymerization activation, deactivation, propagation, and termination, respectively; adapted from ref 5).

Received: May 31, 2012
Published: September 28, 2012

   dx.doi.org/10.1021/ic3011585 | Inorg. Chem. 2012, 51, 10762−10773

of the halide-capped dormant polymers permits use of these products as macroinitiators for the syntheses of block copolymers. Since the original publications, catalysts based on a number of metals have been reported, including systems with titanium, iron, ruthenium, rhodium, nickel, palladium, and copper.[11,13,14] In each case, halide exchange between the metal and the growing polymer chain results in a formal oxidation state change at the metal center. The criteria for an efficient ATRP catalyst thus include the ability of the metal complex to undergo a reversible one-electron redox process at a suitable potential and allow for facile halogen atom transfer. Studies relating the structures of copper complexes to their effectiveness in mediating ATRP have been reviewed.[13,15]

Haddleton et al. employed bidentate 2-iminopyridine complexes of copper(I) [$Cu(L)_2Br$] (e.g., L = *N*-(*n*-pentyl)-2-pyridylmethanimine) in the ATRP of methyl methacrylate and styrene to generate product polymers with good molecular weight control and low polydispersities.[1,16] Other groups have also successfully investigated the use of higher denticity pyridine–amine ligands such as *N*,*N*,*N*′,*N*′-tetrakis(2-pyridylmethyl)ethylene diamine (TPEN) and *N*,*N*,*N*′-tris(2-pyridylmethyl)-*N*′-methylethylenediamine (TPMEN) for use in copper(I)-mediated ATRP.[17,18] In related work carried out in the Gibson laboratories, the efficiency of iron(II) complexes of closely related bidentate and tridentate salicyladiminato ligands in controlling radical polymerizations of styrene was compared.[19] Tridentate ligands were designed by addition of a third nitrogen donor moiety (amine or pyridine) to the framework of the bidentate ligands. Iron complexes of these tridentate ligands were significantly more effective at mediating rapid and well-controlled polymerization of styrene.

Given the preference of copper(I) to form tetrahedral complexes, we applied the concept of extending a bidentate framework to the design of tridentate ligands by investigating copper complexes of tridentate ligands closely related to Haddleton's bidentate 2-iminopyridine ligands to mediate ATRP. The bidentate ligand framework was extended by addition of a third donor to the ligand scaffold, in particular, amine nitrogens for ligands **L1** and **L4**, an ether oxygen in **L2**, and a thioether sulfur donor atom in **L3** (Scheme 1). In addition, conceptual reduction of the central imine functionality to an amine generated another variant in **L5**. In the complex, the fourth coordination site is occupied by a bromide ion to generate neutral copper complexes expected to provide favorable solubilities in the nonpolar medium usually employed in the ATRP of styrene. Herein, we present the syntheses and characterization of the copper(I)–bromide complexes of these five tridentate ligands (**C1**–**C5**, Scheme 2) and a study of their effectiveness in mediating ATRP, with an emphasis of examining how changes in ligand structure impact the properties and performance of the complexes. Structural characterization of these complexes illustrates how small changes in the ligand structure lead to diverse structural motifs in the solid state.

Scheme 1. Conceptual Framework Used in the Choice of Ligands Investigated

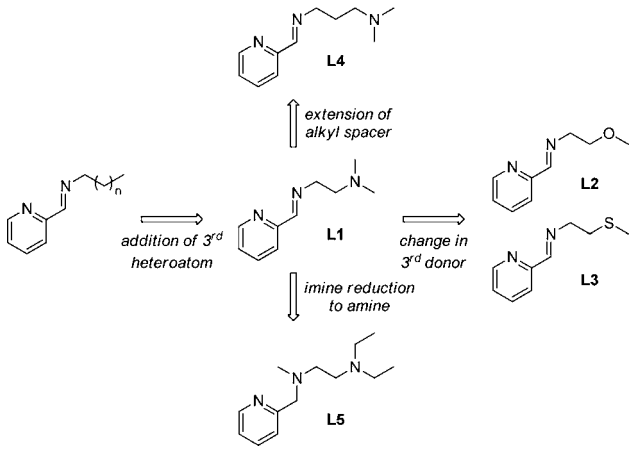

Scheme 2. Synthesis of CuBr Complexes of Ligands L1–L5

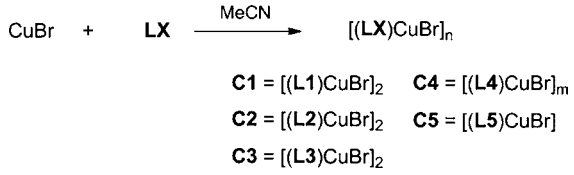

RESULTS AND DISCUSSION

Syntheses of Ligands and Complexes. The syntheses of ligands **L1**–**L5** followed modifications of previously published protocols and proceeded in moderate to excellent yields.[1,20–23] Reaction of ligands with suspensions of CuBr in acetonitrile led to immediate color changes and rapid formation of the respective metal complexes with concomitant dissolution of the metal precursor. Isolated yields for the complexes ranged from 60% to 77%.

Complexes **C1**–**C5** were readily generated in situ by addition of equimolar amounts of ligand to suspensions of CuBr in d_3-acetonitrile. NMR spectra identical to those obtained by dissolving isolated complexes were obtained (vide infra).

Solid State Structures of Copper Complexes. ORTEP representations of the solid state structures of complexes **C1**–**C5** are shown in Figures 2–6. Crystallographic data are provided in Table 1, and selected bond lengths and angles are given in Table 2. Complete structure tables are provided in the Supporting Information. The copper ions in complexes **C1**–**C5** possess distorted tetrahedral geometries. In complexes **C1**–**C4**, two coordination sites are occupied by bidentate pyridine–imine moieties forming planar 5-membered chelate rings. These chelate planes also include the pyridine rings and the

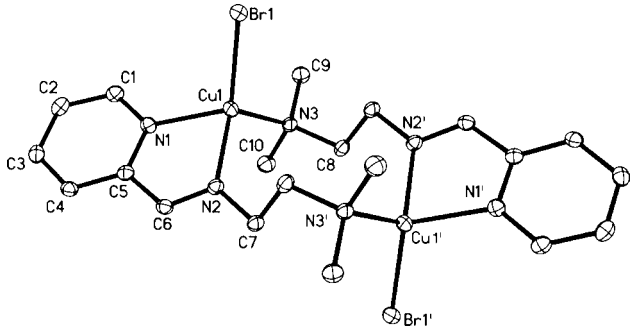

Figure 2. Structure of complex **C1**, the $[(L1)CuBr]_2$ dimer (**L1** = *N*,*N*-dimethyl-*N*′-((pyridin-2-yl)methylene)ethane-1,2-diamine). Thermal ellipsoids are represented at 50% probability (symmetry codes i = $-x$, $-y$, $-z$). Hydrogen atoms are omitted for clarity.

dx.doi.org/10.1021/ic3011585 | *Inorg. Chem.* 2012, 51, 10762–10773

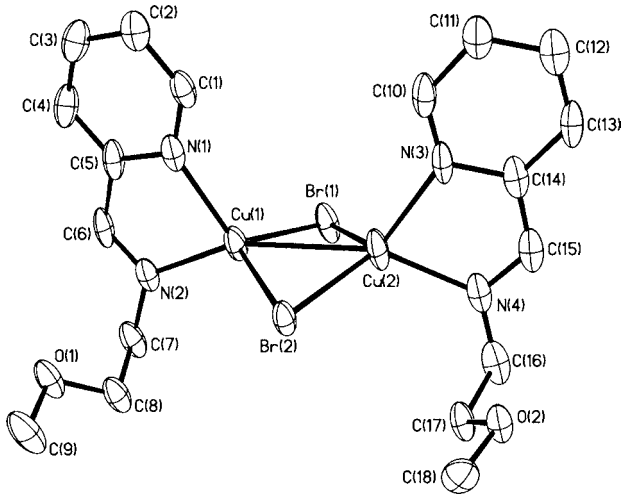

Figure 3. Structure of complex **C2**, the $[(\mathbf{L2})_2Cu_2(\mu\text{-}Br)_2]_2$ dimer (**L2** = 2-methoxy-*N*-((pyridin-2-yl)methylene)ethanamine). Thermal ellipsoids are represented at 50% probability. Hydrogen atoms and solvent molecules are omitted for clarity.

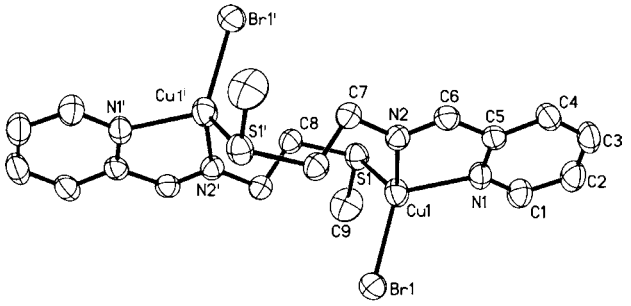

Figure 4. Structure of complex **C3**, the $[(\mathbf{L3})CuBr]_2$ dimer (**L3** = 2-(methylthio)-*N*-(pyridin-2-ylmethylene)ethanamine). Thermal ellipsoids are represented at 50% probability (symmetry codes i = $-x$, $-y$, $-z$). Hydrogen atoms are omitted for clarity.

first carbon atom of the alkyl pendent arms that contain the third donor. In the chelate ring, the copper−imine bond is generally shorter than the copper−pyridine bond, with Cu−N(py) distances ranging from 2.086 to 2.104 Å and Cu−N(im) distances from 2.054 to 2.087 Å. These distances are close to the values expected.[24] N(py)−Cu−N(im) angles are significantly smaller than the ideal tetrahedral angle and range from 79.67° to 80.34°, leading to considerable distortion of the tetrahedral geometry and an opening of other angles. This bite angle is similar to that found in Cu(I) complexes with bidentate pyridyl−imine complexes, where the angles range from 79.4° to 82.3°,[24,25] and in Cu(II) complexes of related tridentate pyridyl−imine ligands, where the angles range from 79.9° to 80.4°.[26,27]

Complexes **C1** and **C3** are structurally similar (Figures 2 and 4, respectively). They crystallize as dimers containing two 5-membered Cu−N(py)−C−C−N(im) chelate rings and a central 10-membered ring formed by two copper ions and two N(im)−C−C−L moieties with the third donor atom of the ligand binding to another copper ion. Despite the presence of an sp^2-hybridized imine *N* in the ring, the configuration of this central 10-membered ring may loosely be described as being in a boat−chair−boat conformation.[28] The inversion center in the center of this ring differentiates the arrangement of this dimeric core from the one found in the double-stranded dicopper(I)

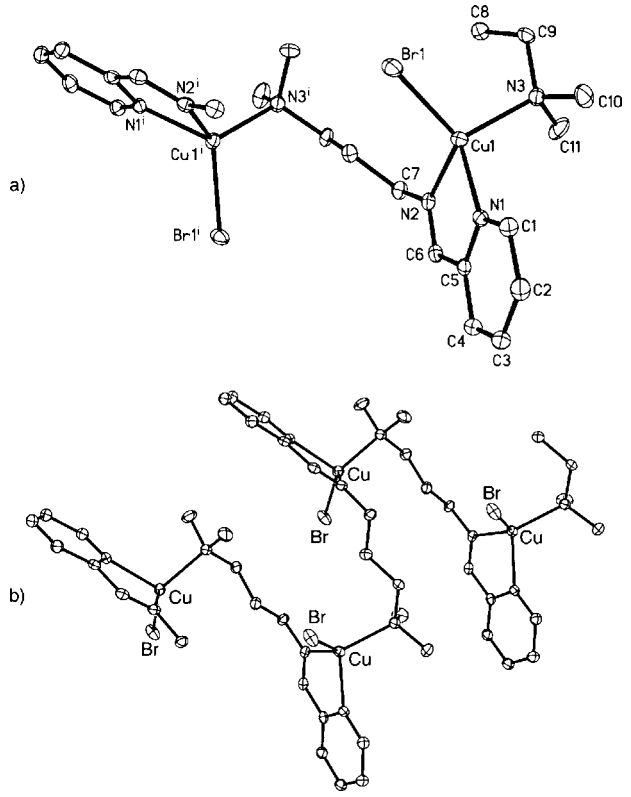

Figure 5. Structure of complex **C4**, the polymeric $[(\mathbf{L4})CuBr]_n$ (**L4** = *N*,*N*-dimethyl-*N*′-(pyridin-2-ylmethylene)propane-1,3-diamine). (a) Dimeric unit of the polymer chain showing binding of a ligand unit to two metal centers. (b) Segment of the polymeric chain illustrating the zigzag arrangement of the polymeric chain. Thermal ellipsoids are represented at 50% probability (symmetry codes i = $-x$, $y + 1/2$, $-z + 1/2$). Hydrogen atoms are omitted for clarity.

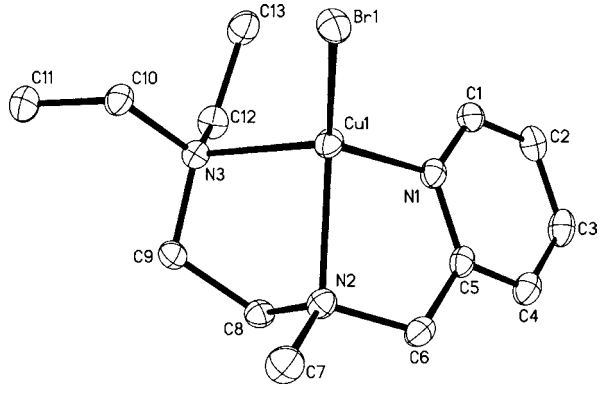

Figure 6. Structure of complex **C5**, the mononuclear [(**L5**)CuBr] (**L5** = *N*,*N*-diethyl-*N*′-methyl-*N*′-(pyridin-2-ylmethyl)ethane-1,2-diamine). Thermal ellipsoids are represented at 50% probability. Hydrogen atoms are omitted for clarity.

helicates of $[Cu_2L_2](PF_6)_2$ (L = *N*,*N*′-bis(6-alkyl-2-pyridylmethylene)ethane-1,2-diamine, where alkyl = H, Me, ^{i}Pr).[29] In these helicate structures, the copper−copper distances range from 3.513 to 3.663 Å, whereas the copper−copper distances found in **C1** and in **C3** are 5.040 and 5.245 Å, respectively. A terminal bromide ion completes the coordination sphere of each copper, with Cu−Br bond distances of 2.3850(4) Å in **C1** and 2.4045(5) Å in **C3** in the range expected for Cu(I)−bromide bonds (mean 2.533 Å, range

dx.doi.org/10.1021/ic3011585 | *Inorg. Chem.* 2012, 51, 10762−10773

Table 1. Crystallographic Data and Structure Refinement for Complexes C1−C5

	C1	C2	C3	C4	C5
formula	$C_{20}H_{30}Br_2Cu_2N_6$	$C_{38}H_{51}Br_4Cu_4N_9O_4$	$C_9H_{12}BrCuN_2S$	$C_{11}H_{17}BrCuN_3$	$C_{13}H_{23}BrCuN_3$
fw (g/mol)	641.40	1271.68	323.72	334.73	364.79
cryst syst	monoclinic	triclinic	monoclinic	orthorhombic	monoclinic
space group	$C2/c$	$P\text{-}1$	$P2_1/n$	$P2_12_12_1$	$P2_1/n$
a (Å)	19.1999(10)	9.5478(2)	7.20090(10)	7.37440(10)	12.0347(2)
b (Å)	10.8924(6)	10.7726(2)	18.5294(3)	13.4167(2)	8.36510(10)
c (Å)	14.1410(8)	11.8274(2)	9.61010(10)	13.9213(2)	15.2742(2)
α (deg)	90.00	89.655(2)	90.00	90.00	90.00
β (deg)	126.285(2)	72.465(2)	110.5270(10)	90.00	98.1120(10
γ (deg)	90.00	84.594(2)	90.00	90.00	90.00
V (Å^3)	2383.9(2)	1154.50(4)	1200.84(3)	1377.38(3)	1522.29(4)
T (K)	100(2)	100(2)	296(2)	100(2)	100(2)
Z	4	1	4	4	4
ρ_{calcd} (g cm^{-3})	1.787	1.829	1.791	1.614	1.592
μ (Cu Kα, mm^{-1})	6.275	6.523	7.795	5.456	4.985
θ range (deg)	4.96−66.98	3.92−58.57	4.77−66.99	4.58−66.99	4.39−66.96
reflns measd	12 895	15 854	12 974	15 082	16 241
independent reflns ([R_{int}])	2067 [0.0333]	3168 [0.0567]	2135 [0.0419]	2407 [0.0337]	2668 [0.0320]
data/restraints/params	267/0/138	3168/1/267	2135/0/128	2407/0/147	2668/0/166
GOF (F^2)	1.014	1.029	1.084	1.089	1.001
R_1/wR_2 [I > 2sigma(I)][a]	0.0188/0.0502	0.0368/0.09168	0.0272/0.0680	0.0173/0.0441	0.0191/0.0524
R indices (all data)	0.0202/0.0510	0.0470/0.0984	0.0290/0.0692	0.0175/0.0442	0.0194/0.0527

[a] $R_1 = \Sigma||F_o| - |F_c||/\Sigma|F_o|$; $wR_2 = [\Sigma\{w(F_o^2 - F_c^2)\}]/\Sigma\{w(F_o^2)^2\}]^{1/2}$.

Table 2. Selected Bond Distances (Angstroms) and Angles (degrees) for Complexes C1−C5

	C1	C2	C3	C4	C5
Cu−Br(1)	2.3850(4)	2.4678[e]	2.4045(5)	2.3842(3)	2.3209(3)
Cu−N(1)[a]	2.0953(15)	2.090[e]	2.096(2)	2.1041(16)	2.0537(14)
Cu−N(2)[b]	2.0700(15)	2.076[e]	2.087(2)	2.0540(16)	2.2112(14)
Cu−L[c]	2.1104(15)	2.4386[e]	2.2810(7)	2.0938(18)	2.1663(14)
C(6)−N(2)[d]	1.276(2)	1.261(7)	1.270(3)	1.273(3)	1.467(2)
Cu(1)−Cu(2)	5.044	2.7298(10)	5.245	6.340	
N(1)−Cu(1)−N(2)	80.25(6)	80.19(17)	79.67(8)	79.74(6)	80.52(5)
N(1)−Cu(1)−L[a,c]	113.42(6)	123.03(11)	113.98(6)	110.51(7)	110.88(5)
N(1)−Cu(1)−Br(1)	110.89(4)	111.85(10)	114.63(6)	116.02(5)	127.41(4)
N(2)−Cu(1)−Br(1)	128.04(4)	111.75(11)	115.82(6)	121.51(5)	128.16(4)
N(2)−Cu(1)−L[c]	107.66(6)	119.38(11)	111.93(6)	116.00(7)	84.00(5)
L[c]−Cu(1)−Br(1)	112.52(4)	108.29(3)	115.77(2)	109.76(5)	114.74(4)
C(6)−N(2)−Cu(1)	112.91(12)	112.9(4)	113.16(16)	114.52(13)	103.74(10)

[a] N(1) is the pyridine N. [b] N(2) is the imine N in **C1**−**C4** and the NMe in **C5**. [c] L = N of NR_2 in **C1** (R = Me), **C4** (R = Me), **C5** (R = Et); L = Br(2) in **C2**; L = S(1) in **C3**. [d] C(6)−N(2) is the imine C═N in **C1**−**C4** and a C−N in **C5**. [e] Average of the following distances shown in table. Cu−Br(1): 2.4601(9) and 2.4758(9) Å. Cu−Br(2): 2.4278(9) and 2.4509(8) Å. Cu−N(1): 2.085(5) and 2.091(5) Å. Cu−N(2): 2.074(4) and 2.075(5) Å.

2.208−2.771 Å).[30] One difference of note between the complexes is that in **C1** the distortions from the tetrahedral angles around copper are more pronounced than in **C3**. In particular, the N(im)−Cu−Br angle of 128° in **C1** is significantly outside the range of angles from 111.9° to 115.8° for **C3**. The Cu−S bond distance of 2.2810(7) Å in **C3** is typical of copper(I)−thioether bonds.[31,32] The closely related copper(I) complex of a tetradentate N_3S ligand, $[Cu(N_3S)]_2[B(C_6F_5)_4]_2$ (N_3S = 2-ethylthio-*N*,*N*-bis(pyridin-2-yl)methylethanamine), forms a dimeric structure similar to **C3**, with Cu−S bond distances of 2.20 Å.[33]

Copper(II) complexes of **L1** have been structurally characterized.[34,35] When additional bridging ligands such as azides were employed, these complexes were investigated for their magnetic properties.[26,27] The coordination geometry of copper(II) ions in these structures is square pyramidal with the nitrogen atoms of the ligand in the basal plane and **L1** roughly planar. In the mononuclear complex $[CuCl_2(\mathbf{L1})]$ the geometry around the copper center is distorted square pyramidal with τ = 0.30 and a Cu−N(py) distance of 2.236(2) Å, a Cu−N(im) distance of 2.104(2) Å, and a Cu−N(am) distance of 2.275(2) Å.[34]

Complex **C2** crystallizes as a doubly-bromide-bridged dimer (Figure 3). The coordination sphere around each copper ion is arranged in a distorted tetrahedral geometry, with ligation by two bridging bromide ions and the two nitrogen atoms of the pyridine−imine ligand. The 5-membered chelate rings of the pyridine−imine units are near planar, and the pyridine rings and the first carbon atom of the ethylene−OMe pendent arms nearly coplanar with the chelate ring. The torsion angle

dx.doi.org/10.1021/ic3011585 | Inorg. Chem. 2012, 51, 10762−10773

between the two pyridine−imine chelate ring planes in the dimer is approximately 13.5°. The Cu_2Br_2 bridging unit forms a near kite-like quadrilateral arrangement, with a Br−Cu−Cu−Br torsion angle of about 156°, resulting in a displacement of about 12° from the idealized Cu_2Br_2 plane. The arrangement of the bromide bridging unit is asymmetrical: one Cu−Br−Cu bridging angle is 67.16(3)° and the other 68.07(2)°. Cu(1) possesses one short (2.4271(8) Å) and one long (2.4753(9) Å) Cu−Br bond, whereas for the second copper center Cu(2) the Cu−Br distances are more similar at 2.4501(8) and 2.4602(8) Å. The Cu(I)−Cu(I) distance is 2.7298(10) Å, indicative of cuprophilic interactions between these formally closed-shell metal centers.[36,37] A search of the Cambridge Structural Database [CSD, Version 5.32 (February 2012)] for structures containing the Cu_2Br_2 bridging unit revealed Cu−Cu distances ranging from about 2.44 to 4.16 Å (mean 3.07 Å) and the Cu−Br−Cu bridging angle ranging from about 50° to 104° (mean 74.9°).[30,38−40] As expected, there is an approximately linear correlation between the bridging angle and the metal to metal separation. The parameters determined for **C2** fall in the lower end for the range of values reported. Similar copper separations are reported for the closely related $[Cu_2Br_2(L)_2]$ complexes of L = 2,2′-bipyridine (Cu−Cu 2.850(1) Å),[41] 2,6-bis-(phenylthiomethyl)pyridine (Cu−Cu 2.728 Å),[42] and *N*,*N*,*N*′,*N*′-tetraethylethylenediamine (Cu−Cu about 2.61 Å).[43] The potential third oxygen donor atom of the ligand of the methyl ether is not involved in bonding to copper. Within the lattice, the ether oxygens display short van der Waals contacts to either the hydrogen of the imine carbon (2.465 Å) or to the hydrogen of the disordered acetonitrile solvent molecule (2.51 Å).

Complex **C4** crystallizes as polymeric chains (Figure 5). Each copper ion is coordinated by a terminal bromide ion and the pyridine and imine nitrogen chelate of one tridentate ligand. The fourth coordination site is occupied by the amine nitrogen of another tridentate ligand (Figure 5a). The closest Cu−Cu separation is about 6.34 Å within the polymeric chain and about 7.37 Å between chains. In the crystal, the polymeric chain is arranged in a zigzag arrangement around the *a* axis of the cell (Figure 5b), with the pyridine−imine chelate ring alternating to either side of the strand. In contrast, the copper(II) bromide structure of this ligand is a mononuclear five-coordinate distorted square pyramid (τ = 0.11), with the tridentate ligand and one bromide ion in the plane and the second bromide in an axial position.[44] The Cu−N bond lengths vary only slightly with the change in oxidation state (Cu−N(py) 2.1041(16)/2.062(2) Å, Cu−N(im) 2.0540(16)/2.036(2) Å, Cu−N(am) 2.0938(18)/2.113(2) Å for the copper(I)/copper(II) species). However, the Cu−Br bond distance is significantly shorter in our copper(I) species at 2.3842(3) Å vis-à-vis 2.4457(5) Å for the in-plane bromide and 2.5940(5) Å for the axial bromide in Sun's structure.

Complex **C5** crystallizes as a mononuclear molecule, with copper in a severely distorted tetrahedral environment (Figure 6). Of the series of complexes examined here, **C5** possesses the shortest Cu−Br bond at 2.3209(3) Å and the shortest Cu−N(py) bond at 2.0537(14) Å. Both Cu−N(amine) bond lengths are long at 2.1663(14) and 2.2112(14) Å but within the range expected for Cu(I)−NR_3 bonds, with 90% of structures falling into the range 1.952−2.274 Å (median 2.112 Å).[30] Notable bond angles leading to the significant distortion of the tetrahedral geometry are the two angles formed by the 5-membered chelate rings N(py)−Cu−N(Me-am) and N(Et_2-am)−Cu−N(Me-am) of 80.52(5)°g and 84.00(5)°, respectively. As a consequence, the N(py)−Cu−Br and N(Me-am)−Cu−Br angles are opened up to 127.41(4)° and 128.16(4)°. The closely related copper(II) complex $[Cu(L)Cl_2]\cdot CH_3OH$ (L = *N*,*N*-dimethyl-*N*′-ethyl-*N*′-(pyridin-2-ylmethyl)ethane-1,2-diamine)[45] was recently characterized by crystallography. The copper(II) ion possesses a distorted square-based pyramidal geometry (τ = 0.02) with the corners of the square plane occupied by the nitrogen atoms of the tridentate ligand and a chloride ion and the apical position occupied by the other chloride ion, resembling the structure of $[CuCl_2(\mathbf{L1})]$. Relative to the copper(I) species, the Cu−N bonds of the copper(II) complex are shortened (Cu−N(py) 2.016(4) Å, Cu−N(amine) at 2.086(4) Å (NEt) and 2.064(4) Å (NMe_2)). The chelate angles remain comparable at 80.52(16)° and 85.67(16)° for the N(py)−Cu−N(Et-am) and N(Me_2-am)−Cu−N(Et-am) angles, respectively.

Further evidence for complexation is the significant change in IR spectra upon binding of the ligand to the metal in **C1**−**C5**. For **C1**−**C4**, the most readily tracked change is in the stretching frequency of the imine, which changes by 20−30 cm^{-1} from about 1650 cm^{-1} in the free ligand to 1620−1630 cm^{-1} in the complexes.

Solution Structure of Copper Complexes. Neutral complexes **C1**−**C5** are soluble in THF or acetonitrile at room temperature and in toluene and styrene at elevated temperatures of about 100 °C. In d_3-acetonitrile solutions the complexes adopt structures resulting in single signals for each type of nucleus in the ^{1}H- and ^{13}C NMR spectra. This observation is consistent with either a symmetric dinuclear or a mononuclear structure for the complexes, including for **C4**. The latter is further supported by electrochemical measurements and is consistent with ESI-mass spectral data (vide infra). As expected for metal-bound ligand, the chemical shifts of the ligand protons and carbons change upon formation of the copper complexes. The azomethine proton chemical shifts, for example, move by between 0.10 and 0.24 ppm for **C1**−**C4**, with corresponding changes in the azomethine carbon chemical shifts in the ^{13}C NMR from 2.4 to 4.7 ppm. Also notable are the relative positions of the chemical shifts for the azomethine hydrogens and the ortho hydrogens of the pyridine rings. For **C1**, for example, the azomethine hydrogen is downfield of the ortho hydrogen, whereas in free ligand **L1** the signal is upfield of the aromatic proton (**L1**: δ 8.64 (*o*-H), 8.34 (N═CH); **C1**: δ 8.60 (N═CH), 8.50 (*o*-H)).

At room temperature, some ^{1}H NMR resonances of the complexes are broadened. This broadening is most notable for **C1**, **C4**, and **C5** (Figure 7 and Supporting Information). At elevated temperatures (up to 333 K), further broadening is observed. However, lowering the temperature of observation to ca. 260 K leads to a reduction in line widths and good resolution for most peaks. For instance, for **C1**, all peaks are well-resolved at this lower temperature and coupling becomes clearly distinguishable (Figure 7). The *o*-H on the pyridine ring at δ 8.5 shows a reduction in line width from about 22 Hz for a broad singlet to 4 Hz for each of the doublet peaks. Similarly, the line width of the NMe_2 peak at δ 3.9 is reduced from approximately 16 to 3 Hz. For **C4** and **C5**, not all signals are resolved at 260 K. For **C4**, the signals associated with the N−$CH_2CH_2CH_2$−N(CH_3)$_2$ fragment remain broad with line widths of 20 Hz. For **C5**, the room-temperature signals show line widths between 20 and 50 Hz, and at 260 K, these values are reduced to between 10 and 20 Hz with unresolved

dx.doi.org/10.1021/ic3011585 | *Inorg. Chem.* 2012, 51, 10762−10773

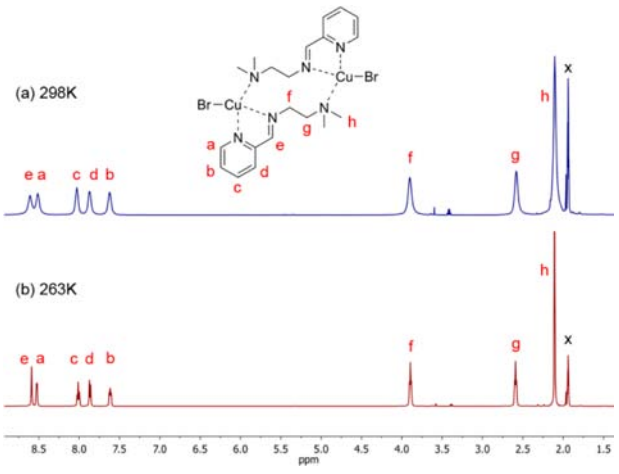

Figure 7. ^{1}H NMR spectra in d_3-acetonitrile of complex **C1**, the $[(\mathbf{L1})CuBr]_2$ dimer (**L1** = *N*,*N*-dimethyl-*N*′-((pyridin-2-yl)-methylene)ethane-1,2-diamine), at 298 (a, blue) and 263 K (b, maroon), showing the broadening of lines at the higher temperature. Assignments are shown (x = acetonitrile solvent).

multiplicities. Lowering the temperature further did not improve the resolution due to precipitation of the complex over the course of the experiment. Ligand exchange on dissolution in combination with conformational exchange and flexibility on the NMR time scale likely lead to broadening of signals.[17,46,47] Comparison across the series of complexes indicates that fluxionality of the pendent arm with the third donor moiety is more prevalent, consistent with the less rigid nature of the sp^3-hybridized carbon spacer, permitting rotation about the single bonds. It is unclear whether rapid interconversions between mono- and dinuclear species also contribute to the broadening.[17,47]

The ESI mass spectra of complexes **C1**−**C4** show the presence of two predominant species in positive ion mode, $[(\mathbf{LX})_2Cu]^+$ and $[(\mathbf{LX})Cu]^+$ (Figure 8 and Supporting Information). The latter is also the major species in the MS-MS spectrum of the $[(\mathbf{LX})_2Cu]^+$ ion. Dinuclear species were largely absent from these spectra. Data are consistent with the break up of the dimeric (**C1**−**C3**) and polymeric solid state (**C4**) structures on dissolution in acetonitrile and ligand exchange to form the bis-ligand copper cation with

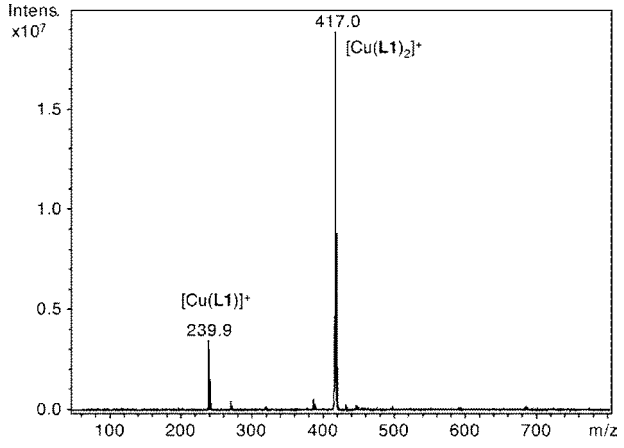

Figure 8. ESI-MS spectrum of complex **C1** dissolved in acetonitrile (**L1** = *N*,*N*-dimethyl-*N*′-((pyridin-2-yl)methylene)ethane-1,2-diamine).

dibromocuprate $[CuBr_2]^-$ as a possible counteranion. The ESI mass spectrum of complexes **C5** (Supporting Information) differs from that of the other complexes and shows the presence of dimeric $[(\mathbf{L5})_2Cu_2Br]^+$ in addition to the $[(\mathbf{L5})Cu]^+$ cation. The latter is also the major species in the MS-MS spectrum of the dimeric cation. The bis-ligand combination $[(\mathbf{L5})_2Cu]^+$ is not detected under the conditions employed. These observations are consistent with formation of a bromide-bridged dinuclear cation, $[((\mathbf{L5})Cu)_2(\mu\text{-Br})]^+$, in acetonitrile solutions of **C5**.

Samples of the complexes of $CuBr_2$ with ligands **L1**−**L5** were generated in situ by reacting equimolar amounts of $CuBr_2$ with the respective ligand in acetonitrile. For analysis by ESI-MS, an equivalent volume of DMF was added after reaction to ensure dissolution of all materials generated. All positive-ion mode ESI mass spectra of these copper(II) complexes show the presence of two species, $[(\mathbf{LX})CuBr]^+$ and $[(\mathbf{LX})_2Cu_2Br_3]^+$ (Figure 9

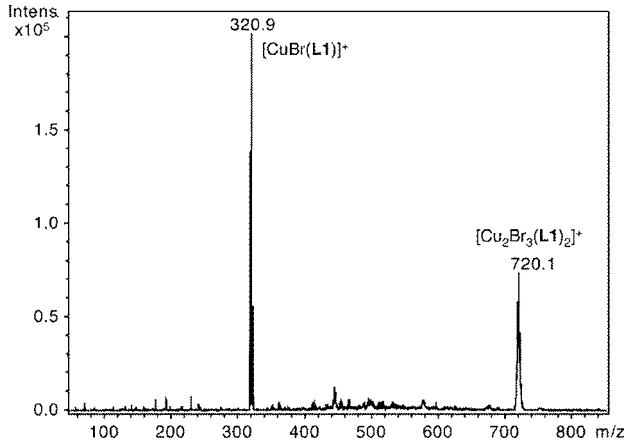

Figure 9. ESI-MS spectrum of an equimolar mixture of $CuBr_2$ and **L1** dissolved in a 1:1 mixture of acetonitrile and DMF (**L1** = *N*,*N*-dimethyl-*N*′-((pyridin-2-yl)methylene)ethane-1,2-diamine).

and Supporting Information). The relative amounts of these cations are generally dependent on the instrument settings. MS-MS spectra of the $[(\mathbf{LX})_2Cu_2Br_3]^+$ ions show major peaks for the $[(\mathbf{LX})CuBr]^+$ ions, consistent with formulation of the dinuclear species as a bromide-bridged dimeric cation, $[((\mathbf{LX})CuBr)_2(\mu\text{-Br})]^+$. For the combination of $CuBr_2$ with ligand **L2**, an additional major peak corresponding to the $[(\mathbf{L2})_2CuBr]^+$ ion is observed. The presence of the bis-ligand formulation is in line with the weaker ether−metal interactions in this complex.

Although **C1**−**C4** possess different solid state structures, the ESI-MS data point to similar solution structures for these complexes, with the possibility of ligand exchange on dissolution often encountered for complexes of metals with d^{10} electron configurations. In studies of other copper complexes used in ATRP, equilibria between mono- and dinuclear complexes have been observed[17,47] and the possibilities of mono- and bis-ligand complexes explored.[46] Electron paramagnetic resonance studies have largely focused on the use of this technique to detect the amount of copper(II) present,[48,49] though recent work by Du Prez et al. identified four different copper(II) species in the ATRP of isobornyl acrylate using *N*,*N*,*N*′,*N*″,*N*″-pentamethyl-diethylene-triamine (PMDETA) as a ligand.[50] Further evidence for the presence of multiple species in ATRP systems has been presented by the

dx.doi.org/10.1021/ic3011585 | Inorg. Chem. 2012, 51, 10762−10773

Matyjaszewski group in a study of the copper halide/PMDETA and tris(2-dimethylaminoethyl)amine (Me_6TREN) systems.[51] The existence of multiple species in solutions of complexes **C1**−**C5** cannot be discounted, particularly at the elevated temperatures of the styrene polymerization.

Redox Potentials of Copper Complexes. Cyclic voltammetry was used to determine the reduction potentials of the complexes in acetonitrile. Cyclic voltammograms are shown in Figure 10, and relevant measurements are provided in

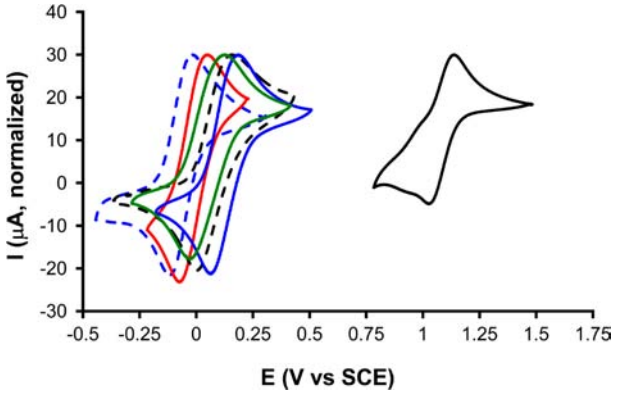

Figure 10. Cyclic voltammograms of complexes **C1**−**C5** and [CuBr/CH_3CN] in acetonitrile with 0.1 M (Bu_4N)(PF_6) supporting electrolyte at a scan rate of 50 mV s^{-1}. Potentials are reported relative to SCE using ferrocene as an internal standard.[60] Key: **C1**, blue dashes; **C2**, black dashes; **C3**, blue; **C4**, green; **C5**, red; [CuBr/CH_3CN], black.

Table 3. Electrochemical Data for the Cu^{II}/Cu^{I} Redox Couple for Complexes C1−C5[a]

	C1	C2	C3	C4	C5
$E_{1/2}$ (V)[b]	−0.07	0.08	0.12	0.02	−0.01
$\Delta E_{1/2}$ (mV)	101	155	114	119	119
i_{pf}/i_{pr}	0.95	0.77	0.95	0.90	0.90
E_{pf} (V)[b]	−0.12	0.00	0.07	−0.04	−0.07
i_{pf} (μA)	12.15	17.76	12.77	14.74	14.74
E_{pr} (V)[b]	−0.02	0.16	0.18	0.08	0.05
i_{pr} (μA)	12.76	23.19	13.41	13.26	13.26

[a]Measurements carried out in MeCN with 0.1 M ($^nBu_4N$)(PF_6) electrolyte, a 0.01 M $AgNO_3$/Ag reference electrode and ferrocene as a reference standard. [b]Potentials are given relative to SCE using the potential of +0.40 V vs SCE for ferrocene as a reference potential for the numeric conversion.

Table 3. The shapes of the voltammograms of the complexes show largely chemically well-behaved redox processes indicative of single species in acetonitrile solutions. Oxidations of the copper(I) complexes **C1** and **C3**−**C5** appear chemically reversible and electrochemically quasi-reversible with the ratios of the forward and reverse currents i_{pf}/i_{pr} between 0.90 and 0.95 and $\Delta E_{1/2}$ values around 100−120 mV. Under identical conditions, the Fc/Fc^+ couple shows a $\Delta E_{1/2}$ of about 70−80 mV and a current ratio i_{pf}/i_{pr} of about 0.95−1.00. The larger than ideal peak-to-peak separations for the complexes are likely the result of the structural reorganization concomitant with the oxidation state change.

For complex **C2**, the peak to peak separation of the forward and reverse scans is increased by about 30 mV to $\Delta E_{1/2}$ = 155 mV and the ratio of the cathodic and anodic currents i_{pf}/i_{pr} is reduced to 0.77. These changes suggest a larger energy associated with structural reorganization of complex **2** upon changing the oxidation state and are consistent with the differences in the species observed in the ESI mass spectra and in the solid state structures obtained for the complexes.

The half-wave potentials for all five complexes studied here fall into a range from −0.07 to +0.12 V. The changes in the third donor atom of this series of tridentate ligands result in a span of variations of about 200 mV in the electrochemical potentials of the copper ion. For example, on substituting the $-NMe_2$ donor moiety (**C1**) with −OMe (**C2**) and −SMe (**C3**) donor groups, the half-wave potentials shift to values 150 and 190 mV more positive for complexes **C2** and **C3**, respectively. The shift on replacing nitrogen donors with thioether donor moieties has been noted previously and attributed to favorable 'soft−soft' copper(I)−thioether interactions and the relative destabilization of the copper(II) species with those ligands.[6,32,52,53] For CuBr dissolved in acetonitrile without additional ligand a chemically and electrochemically quasi-reversible oxidation was observed at +1.08 V ($\Delta E_{1/2}$ = 108 mV, i_{pf}/i_{pr} = 0.91).[54] In addition to this major peak, shoulders at about E_p = 0.55 and 0.70 V indicate that other minor solvated CuBr species exist in solution. Different species are also observed in the solid state structures obtained for CuBr−acetonitrile adducts.[40] As expected, binding of ligands **L1**−**L5** shifted the redox potential to more negative values, with the ligands stabilizing the copper(II) state relative to the solvated forms of CuBr by about 1 V.

The reversible halogen transfer between copper complex and growing polymer chain and concomitant oxidation state change of the metal are central to ATRP, and the relationship between the redox potential of the copper complexes employed and their catalytic activities have been explored.[47,51,54−57] For a series of copper complexes of ligands with N donors (amines and pyridine), a generally linear correlation between the ATRP activity of these complexes and the half-wave potentials was established in the range from about +0.1 V to −0.3 V vs SCE with more negative potentials leading to more active catalysts.[3] The half-wave potentials of the five complexes studied here fall into this range. The following list relates our complexes to copper complexes described in previous studies with comparable potentials: **C1** is similar to copper complexes of 4,4′-di-(5-nonyl)-2,2′-bipyridine (dNbpy) and *N*,*N*-bis[(2-pyridyl)methyl]-propylamine (BPMPA), **C2** is similar to copper complexes of 2,5,9,12-tetramethyl-2,5,9,12-tetraazatridecane (N4[2,3,2]) and 2,6,9,13-tetramethyl-2,6,9,13-tetraazatetradecane (N4[3,2,3]), **C4** is similar to copper complexes of 2,2′-bipyridine (bpy), and **C5** is similar to copper complexes of 1,1,4,7,10,10-hexamethyltriethylenetetramine (HMTETA).[55] The potential for **C3** is more positive than any of the catalysts listed.

Upon extending the spacer arm from an ethylene bridge in **C1** to a propylene bridge in **C4**, the half-wave potential shifts to a value 90 mV more positive. This positive shift has also been observed in complexes of HMTETA (all ethylene spacers) to N4[2,3,2] (one propylene linking unit, shift in potential +0.10 V)[55] and in a series of copper complexes of tripodal mixed pyridine−thioether ligands, where increasing the linkers between the central nitrogen atom and the pyridine nitrogen donor from two to three carbon atoms leads to shifts ranging from +0.13 to +0.21 V.[32,33]

Radical Polymerization of Styrene. Complexes **C1**−**C5** were employed in polymerization of styrene initiated by 1-phenylethyl bromide (1-PEBr) at 110 °C under a nitrogen atmosphere. First-order rate plots of $\ln([M]_0/[M]_t)$ vs time were found to be linear for polymerizations involving complexes **C1**−**C5** (Figure 11). The linearity of the rate

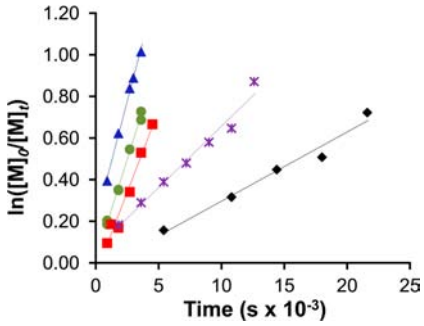

Figure 11. Kinetic plot of $\ln([M]_0/[M]_t)$ vs time (s) for bulk polymerization of styrene using complexes **C1** (▲), **C2** (◆), **C3** (*), **C4** (●), and **C5** (■). Reaction conditions: initial molar ratios Cu:Sty:PEBr = 1:100:1, neat styrene, 110 °C.

plots is consistent with constant radical concentrations throughout the polymerization with limited chain termination events, indicative of living polymerizations of styrene. The nature of the ligand impacts the rate of polymerization, with complexes **C1**, **C4**, and **C5** mediating polymerization at similar rates of $k_{obs} = 2.31 \times 10^{-4}$ s^{-1}, $k_{obs} = 1.92 \times 10^{-4}$ s^{-1}, and $k_{obs} = 1.57 \times 10^{-4}$ s^{-1}, respectively. Polymerization proceeds at a slower rate for complexes **C2** and **C3** with apparent rate constants of $k_{obs} = 3.32 \times 10^{-5}$ and 5.89×10^{-5} s^{-1}, respectively. To provide a comparison to the systems using bidentate 2-iminopyridine complexes of copper employed by Haddleton, the ATRP of styrene using the in-situ-generated 2:1 complex of *N*-hexyl-(2-pyridyl)methanimine of CuBr was carried out under our polymerization conditions. An apparent rate constant of $k_{obs} = 2.42 \times 10^{-5}$ s^{-1} was obtained. Thus, all five tridentate complexes polymerize styrene at rates faster than the bidentate parent complex.[1]

Complexes **C2** and **C3** show the most positive half-wave potentials in this series of complexes, at $E_{1/2}$ (**C2**) = 0.08 V and $E_{1/2}$ (**C3**) = 0.12 V. As a group, the redox potentials of complexes **C1**, **C4**, and **C5** are lower than those of **C2** and **C3** by about 60−190 mV with values of $E_{1/2}$ (**C1**) = −0.07 V, $E_{1/2}$ (**C4**) = 0.02 V, and $E_{1/2}$ (**C5**) = −0.01 V. These lower potentials lead to the relative stabilization of the copper(II) complexes during polymerization for this trio of complexes, consistent with the equilibrium of dormant and active chains favoring formation of active chain ends and hence an increase in the rates of polymerization. However, within the trio, the order of apparent rate constants does not exactly follow the order of redox potentials. **C4** shows slightly higher rates of polymerization despite having more a positive redox potential than **C5**. A possible explanation of the observed rate rankings may lie in the existence of multiple species in solution at 110 °C, the temperature of polymerization. Variations in the composition of these species between **C1** and **C5** would lead to relative reactivities different from those expected from the room-temperature measurement of the potentials.

The number-averaged molecular weights M_n of the polystyrene products increase with conversion for all five complexes (Figures 12−14), as expected for living catalysts. For **C5**, experimental molecular weights closely match theoretical

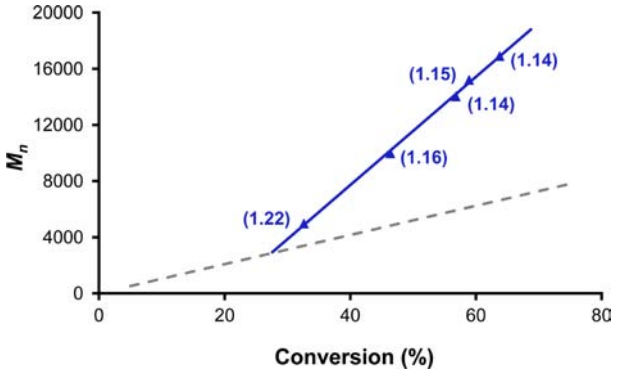

Figure 12. Plot of polystyrene molecular weight M_n vs conversion (%) for bulk polymerization of styrene using complex **C1** (▲). Reaction conditions: initial molar ratios Cu:Sty:PEBr = 1:100:1, neat styrene, 110 °C. Polydispersities (M_w/M_n) are reported in parentheses; theoretical M_n values shown as a dashed gray line.

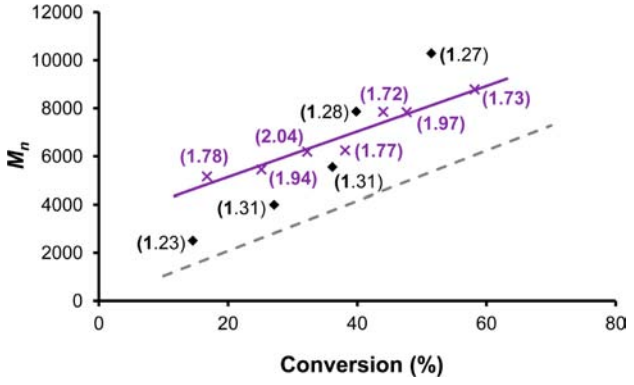

Figure 13. Plot of polystyrene molecular weight M_n vs conversion (%) for bulk polymerization of styrene using complexes **C2** (◆) and **C3** (×). Reaction conditions: initial molar ratios Cu:Sty:PEBr = 1:100:1, neat styrene, 110 °C. Polydispersities (M_w/M_n) are reported in parentheses; theoretical M_n values shown as a dashed gray line.

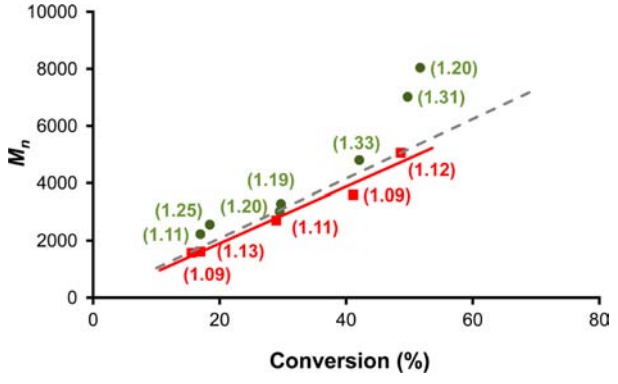

Figure 14. Plot of polystyrene molecular weight M_n vs conversion (%) for bulk polymerization of styrene using complexes **C4** (●) and **C5** (■). Reaction conditions: initial molar ratios Cu:Sty:PEBr = 1:100:1, neat styrene, 110 °C. Polydispersities (M_w/M_n) are reported in parentheses; theoretical M_n values shown as a dashed gray line.

values, with PDI values ranging from 1.09 to 1.13. For **C1**, **C2**, and **C4**, deviations from theoretical molecular weights occurred. Higher than expected molecular weights are obtained,

dx.doi.org/10.1021/ic3011585 | *Inorg. Chem.* 2012, 51, 10762−10773

with reasonably narrow PDIs ranging from 1.14 to 1.22 for **C1** and increased PDIs from 1.23 to 1.31 for **C2** and from 1.11 to 1.35 for **C4**. Contributing factors to these deviations include initiator inefficiencies and the increased viscosity of the polymerization medium as conversions increase. For **C3**, experimental molecular weights are consistently higher by about 3 kDa, with much increased PDIs of 1.72−2.04. These high molecular weight distributions may be indicative of at least two competing processes during polymerization mediated by **C3**: controlled ATRP that is operative for the other complexes of this series and possible chain transfer mediated by the thioether moiety of the ligand.

Of the series of complexes presented here, complexes **C1** and **C5** mediate the controlled polymerization of styrene under the conditions studied in a rapid fashion. Polymerizations conducted with **C1** show a deviation from the theoretical molecular weight growth curve but produce polymer products of narrow polydispersities. Use of **C5** in controlling styrene polymerization yields product with well-controlled molecular weights and low polydispersities.

CONCLUSION

The syntheses and characterization of copper(I) bromide complexes of five tridentate (N,N,L) pyridine−imine and pyridine−amine ligands are presented. Their ligand design illustrates a systematic approach to development of copper complexes for use in ATRP. Changes in the ligand framework lead to interesting and diverse solid state structures. Four of the five tridentate (N,N,L) pyridine−imine and pyridine−amine complexes mediate the living radical polymerization of styrene. As expected from work in other groups, the redox potential of a complex is one indicator of ATRP efficiency. Inherent in the measurement of this potential are geometric changes that accompany the redox process. Complexes with more negative redox potentials tend to mediate ATRP at faster rates without loss of control. Of the series of complexes examined, **C1** and **C5** in particular provide fast polymerization rates and good to excellent molecular weight control and represent important additions to the suite of existing ATRP catalysts.

EXPERIMENTAL SECTION

General Information. Ligand syntheses were conducted in air unless otherwise indicated, and all metal complex syntheses and polymerizations were performed under a dinitrogen atmosphere using standard Schlenk techniques or a MBraun Labmaster SP glovebox. Materials were purchased from commercial sources and used without further purification unless otherwise indicated. Solvents for complexation and polymerization were obtained from a solvent purification system (toluene, tetrahydrofuran, and diethyl ether)[58] or dried using standard techniques (acetonitrile).[59] Styrene (Aldrich, 99%) was run through an activated basic alumina column prior to use, degassed, and stored under a dinitrogen atmosphere at −25 °C.

Characterization. NMR spectra were recorded using a Bruker Avance 500 MHz spectrometer. Chemical shifts are given in ppm relative to residual solvent peaks ($CDCl_3$ ^{1}H NMR δ 7.26 ppm; CD_3CN ^{1}H NMR δ 1.96 ppm, ^{13}C NMR δ 118.69). Assignments are based on collecting combinations of ^{1}H, ^{13}C, COSY and HMQC spectra. FT-IR spectra were obtained with a Perkin-Elmer Spectrum One spectrometer. Complexes were examined using KBr pellets and ligands using NaCl plates. Absorption data were recorded with a Hewlett-Packard 8425A Diode Array spectrophotometer. GC-MS-FID data were collected on an Agilent Technologies 7890A GC system fitted with a HP-5MS column (30 m × 0.25 mm × 0.25 μm), an Agilent 7693 autosampler, and an Agilent 5795C XL EI/Cl MSD and a FID. Electrospray mass spectra were recorded in positive-ion mode using a Bruker Esquire 3000 Plus instrument, and theoretical isotope patterns were obtained with Bruker Daltonics IsotopePattern software. Samples of the complexes of $CuBr_2$ with ligands **L1**−**L5** were generated in situ by reacting equimolar amounts of $CuBr_2$ with the respective ligand **LX** in acetonitrile. Prior to the ESI-MS measurements, equivalent volumes of DMF were added to the reaction mixtures to ensure dissolution of all materials generated, yielding blue-green solutions. Elemental analyses for C, H, and N were obtained from Columbia Analytical Services, Tucson, AZ.

Cyclic voltammetry measurements were carried out using a BASi Epsilon Electrochemical Workstation and the associated Epsilon-EC software. These electrochemical experiments were performed at room temperature in a glovebox under a dinitrogen atmosphere using a BASi VC-2 voltammetry cell with a platinum working electrode (1.6 mm diameter), a platinum wire auxiliary electrode, and a nonaqueous silver/silver ion reference electrode. The reference electrode contained a silver wire immersed in a solution of 0.01 M silver nitrate dissolved in a 0.1 M solution of $(Bu_4N)(PF_6)$ in acetonitrile. Scan rates were varied from 200 to 20 mV s^{-1} with values reported at 50 mV s^{-1}. To facilitate comparisons to electrochemical measurements made by other research groups, potentials are reported relative to the Standard Calomel Electrode (SCE). To convert the values obtained with the silver reference electrode to potentials relative to SCE, the position of the ferrocenium/ferrocene couple was determined under the experimental conditions employed using ferrocene as an internal standard.[60] Values for $E^\circ_{Fc_+/Fc}$ ranged from 0.085 to 0.117 V ($\Delta E_{1/2}$ ranges 73−80 mV; i_{pf}/i_{pr} ranges 0.95−1.00) versus the Ag^+/Ag reference electrode employed. Potential values versus SCE were then calculated using a value of $E^\circ_{Fc_+/Fc}$ = 0.40 V vs SCE in acetonitrile using $(Bu_4N)(PF_6)$ as an electrolyte.[61] Cyclic voltammograms of approximately 1 mM solutions of free ligands **L1**−**L5** and CuBr were determined as controls. Ligands **L2**, **L3**, and **L5** do not display electrochemical activity in the potential range scanned (from −1.0 to +1.3 V). Ligands **L1** and **L4** show irreversible oxidations from about +1.1 to +1.2 V.

Ligand Syntheses. *N,N-Dimethyl-N′-((pyridin-2-yl)methylene)-ethane-1,2-diamine (L1).* **L1** was synthesized by modification of a previously published protocol.[21] *N,N*-Dimethylethane-1,2-diamine (3.62 g, 41.1 mmol) was added to a stirred solution of pyridine-2-carboxaldehyde (4.00 g, 37.3 mmol) in 15 mL of diethyl ether. Anhydrous magnesium sulfate was added. After 4 h of stirring under a dinitrogen atmosphere, the mixture was filtered and solvent and unreacted amine removed from the filtrate under reduced pressure to yield 6.0 g (91% yield) of pure product as a yellow oil. ^{1}H NMR ($CDCl_3$): δ 8.64 (d, J = 4.8 Hz, 1H, py), 8.34 (s, 1H, N═CH), 7.95 (d, J = 7.9 Hz, 1H, py), 7.79 (dd, J = 7.6, 7.9 Hz, 1H, py), 7.37 (dd, J = 4.8, 7.6 Hz, 1H, py), 3.73 (t, J = 6.6 Hz, 2H, NCH_2), 2.57 (t, J = 6.6 Hz, 2H, NCH_2), 2.21 (s, 6H, NCH_3) ppm. ^{13}C NMR (CD_3CN): δ 163.89 (C═N), 156.20 (py), 150.80 (py), 138.00 (py), 126.14 (py), 121.73 (py), 60.93 (NCH_2), 60.24 (NCH_2), 46.25 (NCH_3) ppm. FTIR (cm^{-1}): 3054 (m), 2942 (vs), 2768 (vs), 1650 (vs), 1587 (s), 1568 (s), 1467 (vs), 1437 (s), 1044 (s), 854 (m), 774 (s), 618 (m). MS: m/z 177 (M^+), 133 ($M - NMe_2^+$), 91 ($M - NCH_2CH_2NMe_2^+$), 58 ($Me_2NCH_2^+$).

2-Methoxy-N-((pyridin-2-yl)methylene)ethanamine (L2). **L2** was prepared in a manner similar to **L1** but using 2-methoxyethylamine as a source of amine.[20] The imine product was isolated as a yellow oil in 89% yield on a multigram scale. ^{1}H NMR (CD_3CN, 263 K): δ 8.60 (d, J = 4.7 Hz, 1H, py), 8.31 (s, 1H, N═CH), 7.94 (d, J = 7.9 Hz, 1H, py), 7.79 (dd, J = 7.4,7.9 Hz, 1H, py), 7.37 (dd, J = 4.9, 7.4 Hz, 1H, py), 3.77 (t, J = 5.3 Hz, 2H, NCH_2), 3.65 (t, J = 5.3 Hz, 2H, OCH_2), 3.39 (s, 3H, OCH_3) ppm. ^{13}C NMR (CD_3CN, 263 K): δ 164.37 (C═N), 155.45 (py), 150.50 (py), 137.81 (py), 126.02 (py), 121.39 (py), 72.48 (OCH_2), 61.48 (NCH_2), 58.83 (OCH_3) ppm. FTIR (cm^{-1}): 3054 (m), 2982 (s), 2890 (vs), 1651 (vs), 1587 (s), 1568 (s), 1468 (vs), 1437 (s), 1123 (vs), 775 (s), 617 (m). MS: m/z 164 (M^+), 119 ($M - CH_2OMe^+$), 92 ($MH - NCH_2CH_2OMe^+$), 78 ($M - CHNCH_2CH_2OMe^+$).

dx.doi.org/10.1021/ic3011585 | Inorg. Chem. 2012, 51, 10762−10773

*2-(Methylthio)-N-(pyridin-2-ylmethylene)ethanamine (**L3**).* **L3** was prepared in a similar manner to **L1** but using 2-(methylthio)-ethylamine as a source of amine. Starting with 5.50 mmol of 2-(methylthio)ethylamine and 5.15 mmol of pyridine-2-carboxaldehyde in 40 mL of diethyl ether, the product was isolated as a pale yellow oil in 86% yield. ^{1}H NMR (CD_3CN, 263 K): δ 8.61 (d, J = 4.8 Hz, 1H, py), 8.34 (s, 1H, N=CH), 7.94 (d, J = 7.9 Hz, 1H, py), 7.79 (dd, J = 6, 7.9 Hz, 1H, py), 7.38 (dd, J = 4.7, 6 Hz, 1H, py), 3.82 (t, J = 6.7 Hz, 2H, NCH_2), 2.78 (t, J = 6.7 Hz, 2H, SCH_2), 2.08 (s, 3H, SCH_3) ppm. ^{13}C NMR (CD_3CN, 263 K): δ 164.19 (C=N), 155.46 (py), 150.56 (py), 137.85 (py), 126.10 (py), 121.47 (py), 61.04 (NCH_2), 35.29 (SCH_2), 15.72 (SCH_3) ppm. FTIR (cm^{-1}): 3053 (s), 2915 (vs), 2838 (s), 1648 (vs), 1587 (s), 1568 (s), 1468 (vs), 1436 (vs), 1046 (s), 992 (s), 775 (s), 742 (m), 617 (m). MS: m/z 179 (M − H$^+$), 133 (M − SMe^+), 106 (MH − $CH_2CH_2SMe^+$), 92 (MH − $NCH_2CH_2SMe^+$).

*N,N-Dimethyl-N′-(pyridin-2-ylmethylene)propane-1,3-diamine (**L4**).* **L4**[23] was prepared in a similar manner to **L1** but using N^1,N^1-dimethylpropane-1,3-diamine as a source of amine. The product imine was isolated as yellow oil in 93% yield. ^{1}H NMR (CD_3CN, 258 K): δ 8.59 (d, J = 4.7 Hz, 1H, py), 8.31 (s, 1H, N=CH), 7.94 (d, J = 7.8 Hz, 1H, py), 7.77 (dd, J = 7.4, 7.8 Hz, 1H, py), 7.35 (dd, J = 4.7, 7.4 Hz, 1H, py), 3.61 (t, J = 6.9 Hz, 2H, NCH_2), 2.29 (t, J = 7.2 Hz, 2H, NCH_2), 2.15, (s, 6H, NCH_3), 1.79−1.72 (m, 2H, CCH_2) ppm. ^{13}C NMR (CD_3CN): δ 163.34 (C=N), 156.28 (py), 150.79 (py), 138.00 (py), 126.12 (py), 121.77 (py), 60.18 (NCH_2), 58.46 (NCH_2), 46.38 (NCH_3), 30.28 (CH_2) ppm. FTIR (cm^{-1}): 3054 (s), 2943 (vs), 2765 (vs), 1648 (vs), 1587 (s), 1568 (s), 1468 (vs), 1436 (vs), 1153 (s), 1043 (vs), 992 (s), 775 (s), 742 (m), 617 (m). MS: m/z 190 (M − H$^+$), 147 (M − NMe_2^+), 119 (M − $CH_2CH_2NMe_2^+$).

*N,N-Diethyl-N′-methyl-N′-(pyridin-2-ylmethyl)ethane-1,2-diamine (**L5**).* **L5** was synthesized using a variation of protocol published for synthesis of tripodal tetradentate nitrogen ligands.[22] Pyridine-2-carboxaldehyde (0.51 g, 4.76 mmol) was added to a stirred solution of *N*,*N*-diethyl-*N*′-methylethane-1,2-diamine (0.395 g, 3.03 mmol) and sodium triacetoxyborohydride (2.52 g, 11.89 mmol) in 100 mL of dichloromethane. After 2 days of stirring under a dinitrogen atmosphere, the reaction was quenched by adding 50 mL of saturated aqueous sodium hydrogen carbonate. The product was extracted with ethyl acetate (3 × 50 mL), and the organic extracts were dried over magnesium sulfate. The mixture was filtered, solvent removed under reduced pressure, and oily residue redissolved in 50 mL of tetrahydrofuran and reacted with potassium hydride (0.25 g, 6.23 mmol). After stirring for 2 h solvent was removed under reduced pressure and the product extracted with pentane (4 × 50 mL). Following filtration, solvent was removed from the extract to yield 227 mg (34% yield) of pure product as a red-brown oil. ^{1}H NMR (CD_3CN, 263 K): δ 8.45 (d, J = 4.8 Hz, 1H, py), 7.69 (dd, J = 7.4, 7.8 Hz, 1H, py), 7.44 (d, J = 7.9 Hz, 1H, py), 7.18 (dd, J = 4.9, 7.4 Hz,1H, py), 3.59 (s, 2H, $pyCH_2$), 2.52 (m, 2H, NCH_2), 2.43 (m, overlapping, 2H, NCH_2), 2.43 (m, overlapping, 4H, NCH_2), 2.18 (s, 3H, NCH_3), 0.92 (t, J = 7.2 Hz, 6H, CCH_3) ppm. ^{13}C NMR (CD_3CN): δ 160.96 (py), 149.80 (py), 137.39 (py), 123.71 (py), 122.97 (py), 65.04 ($pyCH_2$), 56.41 (NCH_2), 51.73 (NCH_2), 47.96 (NCH_2), 43.28 (NCH_3), 12.34 (CCH_3) ppm. FTIR (cm^{-1}): 3052 (m), 2968 (s), 2805 (vs), 1590 (vs), 1570 (s), 1472 (vs), 1434 (vs), 1383 (s), 1361 (s), 1293 (m), 1202 (m), 1124 (s), 1047 (vs), 994 (m), 757 (vs), 614 (m). MS: m/z 221 (M$^+$), 135 (M − $CH_2NEt_2^+$), 86 ($Et_2NCH_2^+$).

Complex Syntheses. *(N,N-Dimethyl-N′-((pyridin-2-yl)-methylene)ethane-1,2-diamine)copper(I) Bromide [(**L1**)CuBr].* [(**L1**)CuBr] (**C1**) was synthesized by mixing a light green suspension of CuBr (217 mg, 1.5 mmol) in 3 mL of acetonitrile with 302 mg of ligand **L1** (1.7 mmol) dissolved in 1 mL of acetonitrile. Addition of ligand resulted in an immediate color change of the solution to dark brown and dissolution of CuBr. The reaction mixture was allowed to stir for 1 h and then filtered. The filtrate was layered with 25 mL of diethyl ether. After 1 day at room temperature, the product crystallized as a dark brown solid. The supernatant was removed, and crystals were washed with ether and dried in vacuo to yield 350 mg of crystalline product (70% yield). Anal. Calcd for $C_{10}H_{15}CuBrN_3$: C, 37.45; H, 4.71; N, 13.10. Found: C, 37.78; H, 4.50; N, 12.93. ^{1}H NMR (CD_3CN): δ 8.60 (s, 1H, N=CH), 8.50 (d, J = 4.7 Hz, 1H, py), 8.01 (dd, J = 7.8, 7.9 Hz, 1H, py), 7.88 (d, J = 7.9 Hz, 1H, py), 7.60 (dd, J = 4.7, 7.8 Hz, 1H, py), 3.89 (t, J = 6.4 Hz, 2H, NCH_2), 2.56 (t, J = 6.3 Hz, 2H, NCH_2), 2.11 (s, 6H, NCH_3) ppm. ^{13}C NMR (CD_3CN): δ 162.82 (C=N), 152.20 (py), 150.54 (py), 139.51 (py), 129.17 (py), 127.66 (py), 60.90 (NCH_2), 58.55 (NCH_2), 46.22 (NCH_3) ppm. FTIR (cm^{-1}): 3048 (m), 2975 (s), 2949 (vs), 2838 (vs), 1622 (m), 1587 (s), 1568 (s), 1461 (vs), 1437 (s), 1290 (s), 1019 (s), 1000 (vs), 937 (s), 852 (s), 780 (s), 508 (s). UV−vis: λ_{max}= 466 nm, ε = 1477 L mol^{-1} cm^{-1}. ESI-MS: m/z 417 ([(**L1**)$_2$Cu]$^+$), 240 ([(**L1**)Cu]$^+$).

*(2-Methoxy-N-((pyridin-2-yl)methylene)ethanamine)copper(I) Bromide [(**L2**)CuBr].* [(**L2**)CuBr] (**C2**) was synthesized by mixing a light green suspension of CuBr (196 mg, 1.4 mmol) in 1 mL of THF with 254 mg of ligand **L2** (1.6 mmol) dissolved in 1 mL of THF. Addition of ligand resulted in an immediate color change of the solution to dark brown. The reaction mixture was allowed to stir for 20 min and then filtered. The filtrate was layered with 15 mL of diethyl ether and stored at −25 °C. After 3 days, the product was isolated as a brown solid by removing the supernatant, washing with ether, and drying in vacuo to yield 331 mg of product (78% yield). Anal. Calcd for $C_9H_{12}CuBrN_2O$: C, 35.14; H, 3.93; N, 9.11. Found: C, 35.41; H, 4.30; N, 9.65. ^{1}H NMR (CD_3CN): δ 8.59 (s, 1H, N=CH), 8.52 (d, J = 5.1 Hz, 1H, py), 8.06 (dd, J = 7.6, 7.8 Hz, 1H, py), 7.84 (d, J = 7.8 Hz, 1H, py), 7.66 (dd, J = 5.1, 7.6 Hz, 1H, py), 3.94 (t, J = 5.2 Hz, 2H, NCH_2), 3.60 (t, J = 5.2 Hz, 2H, OCH_2), 3.14 (s, 3H, OCH_3) ppm. ^{13}C NMR (CD_3CN): 163.74 (C=N), 153.19 (py), 150.59 (py), 139.24 (py), 128.60 (py), 126.44 (py), 72.74 (OCH_2), 60.74 (NCH_2), 59.06 (OCH_3) ppm. FTIR (cm^{-1}): 2978 (m), 2910 (vs), 2811 (s), 1634 (s), 1589 (vs), 1564 (m), 1466 (s), 1435 (vs), 1297 (vs), 1124 (s), 1106 (vs), 1023 (s), 952 (m), 840 (s), 772 (s), 633 (m), 502 (s). UV−vis: λ_{max} = 464 nm, ε = 1145 L mol^{-1} cm^{-1}. ESI-MS: m/z 391 ([(**L2**)$_2$Cu]$^+$), 227 ([(**L2**)Cu]$^+$).

*(2-(Methylthio)-N-(pyridin-2-ylmethylene)ethanamine)copper(I) Bromide [(**L3**)CuBr].* [(**L3**)CuBr] (**C3**) was synthesized by mixing a light green suspension of CuBr (434 mg, 3.03 mmol) in 5 mL of acetonitrile with 598 mg of ligand **L3** (3.32 mmol). Addition of ligand resulted in an immediate color change to brown-orange. Stirring overnight led to precipitation of 500 mg of a brown-red solid. The solid was collected by filtration and dried. Layering the supernatant with 7 mL of diethyl ether and storage over 3 days led to formation of brown-orange crystalline material. This solid was isolated and washed with ether to give an additional crop of 150 mg of crystalline product with a combined yield of 66%. Anal. Calcd for $C_9H_{12}CuBrN_2S$: C, 33.39; H, 3.74; N, 8.65. Found: C, 33.71; H, 3.57; N, 8.42. ^{1}H NMR (CD_3CN): δ 8.61 (s, 1H, N=CH), 8.54 (d, J = 5.2 Hz, 1H, py), 8.05 (m, 1H, py), 7.85 (d, J = 7.3 Hz, 1H, py), 7.64 (m, J = 5.2 Hz, 1H, py), 4.01 (t, J = 6.7 Hz, 2H, NCH_2), 2.82 (t, J = 6.7 Hz, 2H, SCH_2), 2.04 (s, 3H, SCH_3) ppm. ^{13}C NMR (CD_3CN): δ 163.37 (C=N), 152.37 (py), 150.69 (py), 139.58 (py), 129.16 (py), 127.53 (py), 59.48 (NCH_2), 36.02 (SCH_2), 15.92 (SCH_3) ppm. FTIR (cm^{-1}): 3046 (s), 2920 (vs), 1630 (s), 1591 (vs), 1563 (s), 1465 (vs), 1444 (vs), 1296 (vs), 1259 (vs), 1147 (s), 1051 (s), 1006 (s), 950 (s), 779 (vs), 693 (m). UV−vis: λ_{max}= 236 nm, ε = 12 200 L mol^{-1} cm^{-1}, λ_{max} = 280 nm, ε = 6320 L mol^{-1} cm^{-1}. ESI-MS: m/z 565 ([(**L3**)$_2$Cu$_2$Br]$^+$), 423 ([(**L3**)$_2$Cu]$^+$), 243 ([(**L3**)Cu]$^+$).

*(N,N-Dimethyl-N′-(pyridin-2-ylmethylene)propane-1,3-diamine)-copper(I) Bromide [(**L4**)CuBr].* [(**L4**)CuBr] (**C4**) was synthesized by reacting a light green suspension of CuBr (580 mg, 4.1 mmol) in 6 mL of acetonitrile with 910 mg of ligand **L4** (4.8 mmol) added dropwise with a pipet. Addition of ligand resulted in an immediate color change of the solution to dark brown and dissolution of CuBr. The reaction mixture was allowed to stir for 2 h and then filtered. The filtrate was layered with 12 mL of diethyl ether and stored at −25 °C for 4 days. After this time, the product crystallized as a brown-black solid. The supernatant was removed, and the crystals were washed with ether and dried in vacuo to yield 1.05 g of crystalline product (77% yield). Anal. Calcd for $C_{11}H_{17}CuBrN_3$: C, 39.47; H, 5.12; N, 12.55. Found: C, 39.84; H, 4.99; N, 12.38. ^{1}H NMR (CD_3CN, 258 K): δ 8.58 (b, 2H, py and N=CH), 8.05 (t, J = 7.7 Hz, 1H, py), 7.82 (d, J = 8.1 Hz, 1H, py), 7.66 (b, 1H, py), 3.88 (b, 2H, NCH_2), 2.27 (b, 2H, NCH_2), 2.10

dx.doi.org/10.1021/ic3011585 | Inorg. Chem. 2012, 51, 10762−10773

(s, 6H, NCH_3), 1.88 (b, 2H, CCH_2) ppm. ^{13}C NMR (CD_3CN, 258 K): δ 161.06 (C═N), 151.51 (py), 150.11 (py), 138.98 (py), 128.82 (py), 127.41 (py), 58.89 (NCH_2), 58.29 (NCH_2), 46.57 (NCH_3), 29.55 (CH_2) ppm. FTIR (cm^{-1}): 3044 (m), 2953 (vs), 2832 (vs), 1621 (s), 1589 (vs), 1465 (vs), 1437 (vs), 1296 (s), 1258 (s), 1178 (s), 985 (s), 840 (s), 777 (vs), 672 (m). UV−vis: λ_{max} = 266 nm (sh), ε = 18 500 L mol^{-1} cm^{-1}, λ_{max} = 374 nm, ε = 3540 L mol^{-1} cm^{-1}, λ_{max} = 456 nm (sh), ε = 1960 L mol^{-1} cm^{-1}. ESI-MS: m/z 445 ($[(\mathbf{L4})_2Cu]^+$), 254 ($[(\mathbf{L4})Cu]^+$).

*(N,N-Diethyl-N′-methyl-N′-(pyridin-2-ylmethyl)ethane-1,2-diamine)copper(I) Bromide [(**L5**)CuBr].* [(**L5**)CuBr] (**C5**) was synthesized by dropwise addition of ligand **L5** (87.1 mg, 0.39 mmol) to a light green suspension of CuBr (56.2 mg, 0.39 mmol) in 1 mL of acetonitrile. This addition of ligand resulted in dissolution of CuBr and an immediate color change of the solution to yellow. The reaction mixture was allowed to stir for 20 min and then filtered. The filtrate was layered with 15 mL of diethyl ether and stored at −25 °C for 2 days. During this time the product crystallized as a yellow solid. Supernatant was removed, and crystals were washed with ether and dried in vacuo to yield 85.7 mg of crystalline product (60% yield). Anal. Calcd for $C_{13}H_{23}BrCuN_3$: C, 42.80; H, 6.36; N, 11.52. Found: C, 43.02; H, 6.25; N, 11.28. ^1H NMR (CD_3CN, 268 K): δ 8.49 (d, J = 8.1 Hz, 1H, py), 7.80 (dd (t), J = 7.7, 7.7 Hz, 1H, py), 7.35 (dd, J = 5.0, 7.7 Hz, 1H, py), 7.32 (d, J = 7.7 Hz, 1H, py), 3.81 (s, 2H, NCH_2), 2.59 (s, 3H, NCH_3), 2.49 (b, 4H, $N(CH_2)_2$), 2.35 (b, 2H, NCH_2), 2.34 (b, 2H, NCH_2), 1.11 (t, J = 7.1, 6H, CCH_3) ppm. ^{13}C NMR (CD_3CN, 258 K): δ 157.65 (py), 149.43 (py), 138.22 (py), 124.79 (py), 124.75 (py), 63.35 (py-CH_2), 54.54 (NCH_2), 52.76 (NCH_2), 48.17 (NCH_2), 44.99 (NCH_3), 10.78 (CCH_3) ppm. FTIR (cm^{-1}): 3059 (m), 2961 (s), 2790 (vs), 1594 (vs), 1565 (s), 1472 (vs), 1435 (vs), 1382 (s), 1367 (s), 1300 (s), 1283 (s), 1107 (s), 1031 (s), 1002 (s), 966 (s), 801 (s), 766 (vs), 737 (s), 595 (m), 526 (m). UV−vis: λ_{max} = 292 nm (sh), ε = 4200 L mol^{-1} cm^{-1}, λ_{max} = 374 nm (sh), ε = 876 L mol^{-1} cm^{-1}. ESI-MS: m/z 649 ($[(\mathbf{L5})_2Cu_2Br]^+$), m/z 284 ($[(\mathbf{L5})Cu]^+$).

General Procedure for Polymerization of Styrene.[1] All reagents were kept under an atmosphere of dinitrogen in a glovebox, and all polymerizations were conducted in the glovebox or on a Schlenk line. Polymerizations of styrene were carried out in bulk and stopped before going to full conversion. For typical polymerization, a 20 mL scintillation vial equipped with a stir bar was charged with about 35 mg of CuBr (0.244 mmol), ligand (0.268 mmol), and styrene (24.4 mmol). The mixture was stirred for 10 min to allow complexation to proceed. The initiator 1-phenylethyl bromide (0.244 mmol, 1 equiv) was added, yielding a 1:1:1.1:100 initiator:metal:ligand:monomer ratio and a target molecular weight of polystyrene product of approximately 10 400 Da at full conversion. The vial was heated to 110 °C on an IKA stir plate fitted with a reactor block. Aliquots were removed at regular time intervals for analysis. Conversion was determined by integration of the monomer vs the polymer backbone resonances in the ^1H NMR spectrum of the crude product in $CDCl_3$.[62]

To determine the molecular weights of a polymer product, an aliquot was added to THF and catalyst removed by passing the solution through a plug of alumina. The resulting filtrate was dripped into methanol to precipitate polymer product. After centrifugation, removal of supernatant, and drying, polymer sample was dissolved to appropriate concentrations in THF and the solution filtered through a 0.45 μm PTFE syringe filter. The molecular weight of this sample was measured by size exclusion chromatography (SEC) analysis at 30 °C using a Waters 1515 isocratic pump, a Waters 2414 refractive index detector, a Waters 2707 autosampler, a Styragel HR3 guard column (Waters), and two PLgel 5 μm MIXED-D columns (Polymer Laboratories) connected in series. Samples were eluted with THF at 1 mL/min. Molecular weights were calculated using polystyrene standards (Agilent) as a reference.

X-ray Crystallography. Crystals suitable for crystallographic analysis were obtained from crystallization from an acetonitrile solution of product and diethyl ether. Crystals were mounted on glass fibers. All measurements were made using graphite-monochromated Cu Kα radiation on a Bruker-AXS three-circle diffractometer equipped with a SMART APEX II CCD detector. Initial space group determination was based on a matrix of 120 frames (SMART Apex II, Data Collection Software, version 2.1; Bruker AXS Inc.: Madison, WI, 2005). Data were reduced using SAINT+ (SAINT Plus, Data Reduction Software, version 7.34a; Bruker AXS Inc.: Madison, WI, 2005) and empirical absorption correction applied using SADABS (Sheldrick, G. M. SADABS; University of Göttingen: Göttingen, Germany, 2005). Structures were solved using direct methods. Least-squares refinement for all structures was carried out on F^2. Non-hydrogen atoms were refined anisotropically. All hydrogen atoms in each structure were located by standard difference Fourier techniques and refined with isotropic thermal parameters. Structure solution, refinement, and calculation of derived results were performed using the SHELXTL package of computer programs.[63] Packing diagrams were produced using Mercury or SHELXP. Details of X-ray experiments and crystal data are summarized in Table 1. Selected bond lengths and bond angles are given in Table 2.

■ ASSOCIATED CONTENT

Ⓢ Supporting Information

Crystallographic data for complexes C1−C5; variable-temperature ^1H NMR spectra for complexes C2−C5; ESI-MS data for C2−C5 and for $[CuBr_2(L)]$ (L = L2− L5). This material is available free of charge via the Internet at http://pubs.acs.org.

■ AUTHOR INFORMATION

Corresponding Author

*E-mail: cgoh@williams.edu.

Notes

The authors declare no competing financial interest.

■ ACKNOWLEDGMENTS

We thank Dr. Emil B. Lobkovsky, Dr. A. Chandrasekaran, and Prof. D. Venkataraman for useful discussions. We acknowledge financial support from the Research Corp. for Science Advancement through RCSA Award 10776 and Williams College for start-up funds and a Hellman Fellowship. We are indebted to NSF (CHE-0443345) and the College of William and Mary for the purchase of the X-ray equipment.

■ REFERENCES

(1) Perrier, S.; Berthier, D.; Willoughby, I.; Batt-Coutrot, D.; Haddleton, D. M. *Macromolecules* **2002**, *35*, 2941.
(2) Cristau, H.-J.; Ouali, A.; Spindler, J.-F.; Taillefer, M. *Chem.—Eur. J.* **2005**, *11*, 2483.
(3) Matyjaszewski, K. *Macromolecules* **2012**, *45*, 4015.
(4) Pintauer, T. *Eur. J. Inorg. Chem.* **2010**, *2010*, 2449.
(5) Pintauer, T.; Matyjaszewski, K. *Chem. Soc. Rev.* **2008**, *37*, 1087.
(6) Lee, Y.; Lee, D.-H.; Park, G. Y.; Lucas, H. R.; Narducci Sarjeant, A. A.; Kieber-Emmons, M. T.; Vance, M. A.; Milligan, A. E.; Solomon, E. I.; Karlin, K. D. *Inorg. Chem.* **2010**, *49*, 8873.
(7) Samanta, B.; Chakraborty, J.; Choudhury, C. R.; Dey, S. K.; Dey, D. K.; Batten, S. R.; Jensen, P.; Yap, G. P. A.; Mitra, S. *Struct. Chem.* **2007**, *18*, 33.
(8) Mukherjee, S.; Gole, B.; Song, Y.; Mukherjee, P. S. *Inorg. Chem.* **2011**, *50*, 3621.
(9) Braymer, J. J.; Merrill, N. M.; Lim, M. H. *Inorg. Chim. Acta* **2011**, *380*, 261.
(10) Matyjaszewski, K.; Tsarevsky, N. V. *Nat. Chem.* **2009**, *1*, 276.
(11) Ouchi, M.; Terashima, T.; Sawamoto, M. *Chem. Rev.* **2009**, *109*, 4963.
(12) Matyjaszewski, K.; Spanswick, J. *Mater. Today* **2005**, *8*, 26.
(13) di Lena, F.; Matyjaszewski, K. *Prog. Polym. Sci.* **2010**, *35*, 959.
(14) Pintauer, T.; Matyjaszewski, K. In *Topics in Organometalic Chemistry*; Guan, Z., Ed.; Springer Berlin: Heidelberg, 2009; Vol. *26*, p 221.

(15) Pintauer, T.; Matyjaszewski, K. *Coord. Chem. Rev.* **2005**, *249*, 1155.
(16) Haddleton, D. M.; Crossman, M. C.; Dana, B. H.; Duncalf, D. J.; Heming, A. M.; Kukulj, D.; Shooter, A. J. *Macromolecules* **1999**, *32*, 2110.
(17) Tang, H. D.; Arulsamy, N.; Radosz, M.; Shen, Y. Q.; Tsarevsky, N. V.; Braunecker, W. A.; Tang, W.; Matyjaszewski, K. *J. Am. Chem. Soc.* **2006**, *128*, 16277.
(18) Zhang, L.; Tang, H.; Tang, J.; Shen, Y.; Meng, L.; Radosz, M.; Arulsamy, N. *Macromolecules* **2009**, *42*, 4531.
(19) O'Reilly, R. K.; Gibson, V. C.; White, A. J. P.; Williams, D. J. *J. Am. Chem. Soc.* **2003**, *125*, 8450.
(20) Klerk-Engels, B. d.; Friibauf, H.-W.; Vrieze, K.; Kooijman, H.; Spek, A. L. *Inorg. Chem.* **1993**, *32*, 5528.
(21) Wei, L.; Babich, J.; Zubieta, J. *Inorg. Chim. Acta* **2005**, *358*, 3691.
(22) Britovsek, G. J. P.; England, J.; White, A. J. P. *Inorg. Chem.* **2005**, *44*, 8125.
(23) Mukherjee, P. S.; Dalai, S.; Mostafa, G.; Lu, T.-H.; Rentschler, E.; Chaudhuri, N. R. *New J. Chem.* **2001**, *25*, 1203.
(24) Dehghanpour, S.; Bouslimani, N.; Welter, R.; Mojahed, F. *Polyhedron* **2007**, *26*, 154.
(25) Haddleton, D. M.; Duncalf, D. J.; Kukulj, D.; Heming, A. M.; J. Shooter, A.; J.; Clark, A. *J. Mater. Chem.* **1998**, *8*, 1525.
(26) Mukherjee, P. S.; Maji; Tapas, K.; Escuer, A.; Vicente, R.; Ribas, J.; Rosair, G.; Mautner, F. A.; Chaudhuri, N. R. *Eur. J. Inorg. Chem.* **2002**, *2002*, 943.
(27) Karmakar, R.; Choudhury, C. R.; Hughes, D. L.; Yap, G. P. A.; El Fallah, M. S.; Desplanches, C.; Sutter, J.-P.; Mitra, S. *Inorg. Chim. Acta* **2006**, *359*, 1184.
(28) Pawar, D. M.; Cain, D.; Gill, G.; Bain, A. D.; Sullivan, R. H.; Noe, E. A. *J. Org. Chem.* **2006**, *72*, 25.
(29) Habermehl, N. C.; Angus, P. M.; Kilah, N. L.; Norén, L.; Rae, A. D.; Willis, A. C.; Wild, S. B. *Inorg. Chem.* **2006**, *45*, 1445.
(30) Bruno, I. J.; Cole, J. C.; Edgington, P. R.; Kessler, M.; Macrae, C. F.; McCabe, P.; Pearson, J.; Taylor, R. *Acta Crystallogr., Sect. B: Struct. Sci.* **2002**, *58*, 389.
(31) Yu, Q.; Salhi, C. A.; Ambundo, E. A.; Heeg, M. J.; Ochrymowycz, L. A.; Rorabacher, D. B. *J. Am. Chem. Soc.* **2001**, *123*, 5720.
(32) Ambundo, E. A.; Deydier, M.-V.; Grall, A. J.; Aguera-Vega, N.; Dressel, L. T.; Cooper, T. H.; Heeg, M. J.; Ochrymowycz, L. A.; Rorabacher, D. B. *Inorg. Chem.* **1999**, *38*, 4233.
(33) Lee, D.-H.; Hatcher, L. Q.; Vance, M. A.; Sarangi, R.; Milligan, A. E.; Narducci Sarjeant, A. A.; Incarvito, C. D.; Rheingold, A. L.; Hodgson, K. O.; Hedman, B.; Solomon, E. I.; Karlin, K. D. *Inorg. Chem.* **2007**, *46*, 6056.
(34) Yuan, W.-B.; Zhang, Q. *Acta Crystallogr., Sect. E: Struct. Rep. Online* **2005**, *61*, M1883.
(35) Yue, G. R.; Xu, X. J.; Shi, Y. Z.; Feng, L. *Acta Crystallogr., Sect. E: Struct. Rep. Online* **2005**, *61*, M693.
(36) Hermann, H. L.; Boche, G.; Schwerdtfeger, P. *Chem.—Eur. J.* **2001**, *7*, 5333.
(37) Pyykkö, P. *Chem. Rev.* **1997**, *97*, 597.
(38) Li, R.; Moubaraki, B.; Murray, K. S.; Brooker, S. *Dalton Trans.* **2008**, *37*, 6014.
(39) Deng, Z.-P.; Qi, H.-L.; Huo, L.-H.; Ng, S. W.; Zhao, H.; Gao, S. *Dalton Trans.* **2010**, *39*, 10038.
(40) Healy, P.; Kildea, J.; White, A. *Aust. J. Chem.* **1989**, *42*, 137.
(41) Skelton, B. W.; Waters, A. F.; White, A. H. *Aust. J. Chem.* **1991**, *44*, 1207.
(42) Ball, R. J.; Genge, A. R. J.; Radford, A. L.; Skelton, B. W.; Tolhurst, V. A.; White, A. H. *J. Chem. Soc., Dalton Trans.* **2001**, 2807.
(43) Churchill, M. R.; Davies, G.; Elsayed, M. A.; Fournier, J. A.; Hutchinson, J. P.; Zubieta, J. A. *Inorg. Chem.* **1984**, *23*, 783.
(44) Sun, Y. X. *Synth. React. Inorg., Met.-Org., Nano-Met. Chem.* **2006**, *36*, 621.
(45) Dhanalakshmi, T.; Suresh, E.; Palaniandavar, M. *Inorg. Chim. Acta* **2011**, *365*, 143.
(46) Levy, A. T.; Olmstead, M. M.; Patten, T. E. *Inorg. Chem.* **2000**, *39*, 1628.
(47) Eckenhoff, W. T.; Pintauer, T. *Inorg. Chem.* **2010**, *49*, 10617.
(48) Kajiwara, A.; Matyjaszewski, K.; Kamachi, M. *Macromolecules* **1998**, *31*, 5695.
(49) Wang, A. R.; Zhu, S. *Macromolecules* **2002**, *35*, 9926.
(50) Caretti, I.; Dervaux, B.; Du Prez, F. E.; Van Doorslaer, S. *J. Polym. Sci., Part A: Polym. Chem.* **2010**, *48*, 1493.
(51) Bortolamei, N.; Isse, A. A.; Di Marco, V. B.; Gennaro, A.; Matyjaszewski, K. *Macromolecules* **2010**, *43*, 9257.
(52) Rorabacher, D. B. *Chem. Rev.* **2004**, *104*, 651.
(53) Bernardo, M. M.; Heeg, M. J.; Schroeder, R. R.; Ochrymowycz, L. A.; Rorabacher, D. B. *Inorg. Chem.* **1992**, *31*, 191.
(54) Qiu, J.; Matyjaszewski, K.; Thouin, L.; Amatore, C. *Macromol. Chem. Phys.* **2000**, *201*, 1625.
(55) Tang, W.; Kwak, Y.; Braunecker, W.; Tsarevsky, N. V.; Coote, M. L.; Matyjaszewski, K. *J. Am. Chem. Soc.* **2008**, *130*, 10702.
(56) Matyjaszewski, K.; Goebelt, B.; Paik, H.-j.; Horwitz, C. P. *Macromolecules* **2001**, *34*, 430.
(57) Peng, C.-H.; Kong, J.; Seeliger, F.; Matyjaszewski, K. *Macromolecules* **2011**, *44*, 7546.
(58) Pangborn, A. B.; Giardello, M. A.; Grubbs, R. H.; Rosen, R. K.; Timmers, F. J. *Organometallics* **1996**, *15*, 1518.
(59) Perrin, D. D.; Armarego, W. L. F. *Purification of Laboratory Chemicals*, 4th ed.; Reed Educational and Professional Publishing Ltd.: Woburn, MA, 2000.
(60) Gagne, R. R.; Koval, C. A.; Lisensky, G. C. *Inorg. Chem.* **1980**, *19*, 2854.
(61) Connelly, N. G.; Geiger, W. E. *Chem. Rev.* **1996**, *96*, 877.
(62) Tillman, E. S.; Contrella, N. D.; Leasure, J. G. *J. Chem. Educ.* **2009**, *86*, 1424.
(63) Sheldrick, G. *Acta Crystallogr., Sect. A: Found. Crystallogr.* **2008**, *64*, 112.